Martian Highland Paterae: Studies of Volcanic and Degradation Histories from High-Resolution Images and Impact Crater Populations. David A. Crown, Daniel C. Berman, Leslie F. Bleamaster, III, Frank C. Chuang, and William K. Hartmann, Planetary Science Institute, 1700 E. Ft. Lowell Rd., Suite 106, Tucson, AZ 85719, crown@psi.edu.

Introduction. A detailed understanding of the chronology of volcanism on Mars is a fundamental goal of planetary exploration that provides critical constraints on surface evolution, magmatic histories of eruptive centers, and the thermal evolution of the lithosphere. New analyses of Martian volcanoes characterize the earliest preserved phase of central-vent volcanism on Mars and contribute to assessments of changes in volcanic style as a function of time, as well as to resurfacing and degradation events that may be related to regional or global geologic evolution. Using MOC and THEMIS images, we are compiling size-frequency distributions of small craters on the Martian highland paterae. As part of this effort, we are examining the variability of small crater populations across geologic units of interest in order to develop a methodology for integrating small crater populations with Viking crater statistics to generate "full" crater size distributions for craters greater than ~10 m in diameter. We use analyses of small-scale surface morphology and comparisons between crater populations on the highland paterae and surrounding units of different ages, types, and settings to determine the nature of crater obliteration and modification processes for the patera surfaces and the Hellas region in general. These studies provide new constraints on the age, duration, internal structure/composition, and erosional history of highland paterae.

Martian Highland Paterae. Formation of low-relief, areally extensive volcanoes with prominent radial valleys has been attributed to voluminous explosive eruptions, potentially due to interactions with a volatile-rich megaregolith [1-4]. The amphitheater-headed flank valleys, layering exposed in valley walls, and erosional remnant mesas observed in Viking images of Hadriaca and Tyrrhena Paterae were attributed to the combined effects of surface runoff and groundwater sapping acting on a sequence of pyroclastic flow deposits [5-7]. Both volcanoes exhibit caldera complexes in their summit regions, and Tyrrhena Patera exhibits a series of rilles, one a lava channel that extends southwest from the summit where it joins a ~1000 km long lava flow field. In MOC and THEMIS images, the small scale characteristics of the caldera-filling deposits, the rille and valley floor deposits, and the upper paterae surfaces can now be reevaluated to assess their origins and relative ages.

Methodology: GIS Database. Central to this project is creation of a Geographical Information Systems (GIS) database, which is used to a) select images for impact crater population studies (to facilitate covering different geologic units, sampling units at different elevations, and selecting images appropriate to cover the "full" crater size range), b) analyze and compare imaging datasets (e.g., day and night THEMIS IR, THEMIS VIS, and MOC narrow-angle images), c) analyze MOLA topography (to evaluate potential elevation-dependent effects on crater preservation), and d) calculate slopes and areas for crater count sites. The GIS database includes Viking MDIM 2.1 and MOLA topography (128 pxl/deg) base layers in simple cylindrical map projection and selected THEMIS and MOC images processed using ISIS software.

Methodology: Crater-Size Distributions. In past studies, Viking images and photomosaics have been used to generate crater statistics for various units of the highland paterae [9-13]. Analyses of crater distributions for diameters > ~1 km were used to assess Martian ages. THEMIS VIS images (~20 m/pxl) provide a straightforward means to extend characterizations of crater populations down to ~200 m. The areal coverage of individual THEMIS VIS images is sufficient to identify geologic units and unit boundaries defined in Viking analyses, such that THEMIS and Viking crater counts can be combined. The high spatial resolution of MOC images (~1.5-10 m/pxl) allows for compilation of crater distributions for craters greater than ~10 m in diameter if sufficient MOC coverage is available. However, the limited areal coverage of an individual MOC image and the small-scale variability of the Martian surface make this more complex and introduce statistical uncertainties.

In order to develop a consistent methodology for generating "full" (MOC-THEMIS-Viking) crater distributions, we compile and compare crater distributions from multiple MOC images of the same unit. If the distributions are similar, the data can be combined to improve statistical characterizations at small sizes by increasing the surface area examined. Multiple MOC images of the major units defined at Hadriaca and Tyrrhena Patera are available in datasets released as of 1/1/05, and there is significant overlap between MOC and THEMIS coverage. Annotated digital images showing all craters included in counts are saved and can be checked and refined, and counts are repeated to assess uncertainties due to the operator. For some units for which MOC counts are obtained, craters are classified as fresh or degraded. Due to recent studies of Martian secondary crater chains extending for large distances from their primary crater [14-15], it is important to analyze MOC images for potential influences by secondary craters. In our analyses, we identify and remove, from our counting areas, any obvious clusters of secondary craters and also attempt to identify the associated primary crater in order to gauge the size range and distances at which age determinations are affected in a significant way.

Results. Initial analyses from crater distributions compiled from 12 MOC images and 5 THEMIS images of Tyrrhena Patera and 4 MOC images and 2 THEMIS images of Hadriaca Patera include the caldera/summit regions and flanks of both volcanoes as well as the floor of the large rille at Tyrrhena Patera (Figure 1). Previous Viking crater statistics were interpreted to indicate a Late Noachian/Early Hesperian and an Early Hesperian age for dissected flanks of Tyrrhena Patera and Hadriaca Patera, respectively [8-12]. However, these studies did not separate counting areas for floors of erosional valleys from the high-standing patera surfaces between them. The timing and spatial variations in flank erosion relative to eruptive activity are not well constrained from Viking crater counts. In THEMIS images, ejecta from craters in the ~5-15 km diameter range appears to superpose both the upper patera surfaces and floors of erosional valleys. Thus, past Viking counts would indicate that both the formation and erosion of the volcanoes are ancient. Plotted together, Viking and THEMIS counts generally match shapes of Martian isochrons developed by Hartmann and Neukum [16-17], with a transition to a steeper slope in the 1-2 km diameter range. Age constraints from craters with diameters between ~250 m and 1 km (counted on THEMIS images) are consistent with earlier Viking results, and THEMIS spatial resolution allows counting areas for heavily cratered patera surfaces to be separated from valley floors, which on Tyrrhena Patera are often covered with dunes and show distinct populations of fresh and degraded craters.

Crater counts from different MOC images for a given unit are generally similar but do show variability that increases toward smaller crater diameters. Results for diameters between ~50 and 250 m clearly show that the patera surfaces are old; saturation equilibrium at small diameters is approached for high-standing Tyrrhena Patera surfaces. Comparisons between counts for high-standing Tyrrhena Patera surfaces and adjacent valley floors show fewer craters on valley floor surfaces and a gradual decrease in the abundance of fresh craters on valley floors as crater diameter decreases, suggesting that the valley floor surfaces are ancient and have undergone progressive degradation, rather than widespread resurfacing. Crater distributions for the floor of the rille extending to the SW from Tyrrhena Patera show, for crater diameters between ~125 and 500 m, a significantly younger surface age than for the flank materials with a gradual loss of craters toward smaller sizes; the crater distributions are consistent with late-stage effusive activity at Tyrrhena Patera [5] and ongoing degradation of lava flow surfaces.

Small crater distributions for Hadriaca Patera indicate old surfaces for both the flanks and caldera floor (Figure 1). Differences between the caldera floor and flank distributions evident at small crater sizes could be due to differences in age [10, 12] and/or to a depletion of craters on the caldera floor due to accumulation of windblown materials or pyroclastic deposits in the topographic low of the caldera. Future work will include continued compilation of crater size-frequency distributions from MOC and THEMIS images, comparisons with surrounding units, and synthesis of small-scale morphologic observations to provide new constraints on the geologic evolution of the highland paterae.

References. [1] Greeley R. and P.D. Spudis (1981) *Rev. Geophys. 19*, 13-41. [2] Francis P.W. and C.A. Wood (1992) *JGR 87*, 9881-9889. [3] Mouginis-Mark P.J. et al. (1992) in *Mars*, Univ. Arizona Press, pp. 424-452. [4] Greeley R. et al. (2000) in *Environmental Effects on Volcanic Eruptions*, Kluwer Academic/Plenum Publishers. [5] Greeley R. and D.A. Crown (1990) *JGR 95*, 7133-7149. [6] Gulick V.C. and V.R. Baker (1990) *JGR 95*, 14,325-14,344. [7] Crown D.A. and R. Greeley (1993) *JGR 98*, 3431-3451. [8] Plescia J.B. and R.S. Saunders (1979) *Proc. LPSC 10*, 2841-2859. [9] Greeley R. and J.E. Guest (1987) *USGS Misc. Invest. Ser. Map, I-1802B*. [10] Crown D.A. et al. (1992) *Icarus 100*, 1-25. [11] Gregg T.K.P. et al. (1998) *USGS Misc. Invest. Ser. Map, I-2556*. [12] Mest S.C. and D.A. Crown (2001) *Icarus, 153*, 89-110. [13] Crown D.A. and R. Greeley (2005) Geologic map of MTM -30262 and -30267 quadrangles, Hadriaca Patera region of Mars, *USGS*, in review. [14] McEwen A.S. et al. (2005) The rayed crater Zunil and interpretations of small impact craters on Mars, *Icarus*, in review. [15] McEwen A.S. et al. (2003) *LPSC XXXIV*, Abstract 2040. [16] Hartmann W.K. and G. Neukum (2001) in *Chronology and Evolution of Mars*, Kluwer Press, pp. 165-194. [17] Hartmann W.K. (2005) Martian cratering 8: Isochron refinement and the chronology of Mars, *Icarus*, in review.

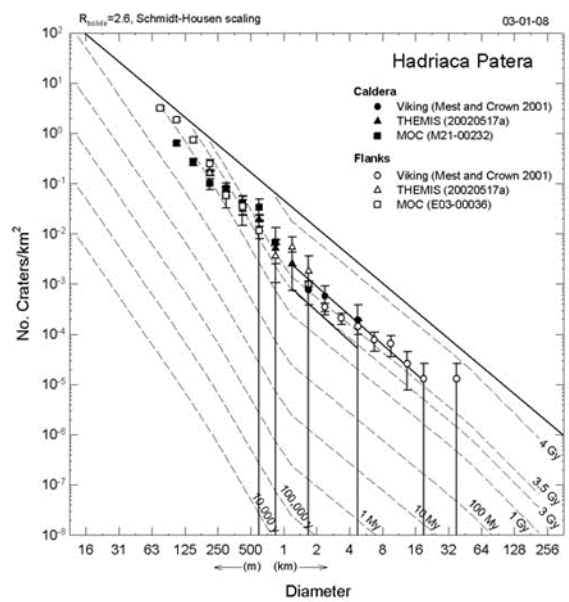

Figure 1. Crater distributions from MOC, THEMIS, and Viking crater counts for Hadriaca Patera flank and caldera floor deposits.